

**AN EFFECTIVE TOOL FOR ENHANCING THE STATIC
BACKCALCULATION OF PAVEMENT MODULI**

Bojan B. Guzina
Assistant Professor
Department of Civil Engineering
University of Minnesota
500 Pillsbury Drive S.E.
Minneapolis, MN 55455
USA
Tel: (612) 626-0789
Fax: (612) 626-7750
Email: guzina@wave.ce.umn.edu

Robert H. Osburn
Undergraduate Research Assistant
Department of Civil Engineering
University of Minnesota
500 Pillsbury Drive S.E.
Minneapolis, MN 55455
USA
Tel: (612) 625-8337
Fax: (612) 626-7750
Email: osbu0002@tc.umn.edu

Submitted to Committee **A2B05** for possible presentation and publication
at 81st Annual Meeting of Transportation Research Board
January 13-17, 2002
Washington, D.C.

AN EFFECTIVE TOOL FOR ENHANCING THE STATIC BACKCALCULATION OF PAVEMENT MODULI

ABSTRACT

The Falling Weight Deflectometer (FWD) test is one of the most commonly used tools for nondestructive evaluation of flexible pavements. Although the test is intrinsically dynamic in nature, the state-of-practice backcalculation techniques that are used to interpret the FWD records are primarily elastostatic-based owing in part to the high computational cost of dynamic multi-layered solutions. It has long been known that the foregoing discrepancy may lead to considerable systematic errors in the estimation of pavement moduli in situations where the inertial and resonance phenomena are pronounced due to the presence of bedrock or seasonal stiff layer. In this investigation, a simple, yet effective algorithm is proposed that allows the static backcalculation analyses to perform well even when dynamic effects are significant. The technique is based on the use of the Discrete Fourier Transform as a pre-processing tool, which filters the dynamic effects and extracts the static pavement response from transient FWD records. With the use of the filtered (i.e. zero-frequency) force and deflection values in lieu of their peak counterparts, the static backcalculation can be further performed in a conventional manner, but free of inconsistencies associated with the neglect of dynamic effects. Illustrative results based on synthetic deflection records demonstrate a marked improvement in the elastostatic prediction of pavement moduli when the proposed modification is used. The filtering algorithm can be implemented on a personal computer as a pre-processor for the conventional FWD data interpretation, requiring only a minimal increase in the computational effort required to backcalculate the pavement moduli.

INTRODUCTION

One of the primary concerns in pavement engineering is the fast and accurate assessment of pavement deterioration owing to its central role in an economic maintenance of roads and highways. Presently, the backcalculation of pavement elastic moduli from the Falling Weight Deflectometer (FWD) measurements is a well-recognized procedure for estimating the pavement integrity. For engineering applications where simplicity is a virtue, elastostatic-based interpretation of the falling weight-induced force and deflection records remains the norm as a tool to estimate the pavement's stiffness characteristics.

Due to the decided dynamic nature of the FWD test, elastostatic backcalculation has long been known to be capable of producing erroneous estimates of the pavement's moduli, especially in the presence of a shallow stiff layer (1-4) which reflects the incident stress waves and distorts the surface deflection records. To deal with the problem, a number of investigations over the past decade have focused on the dynamic interpretation of FWD data [e.g. (3), (5-6)]. Beyond introducing consistency into the reading of transient deflection records, dynamic back-analyses provide more physical insight into the pavement section by (i) exploiting phenomena such as wave reflection, refraction, and dispersion, and (ii) taking into account the viscoelastic nature of asphalt concrete. Despite its advantages in resolving the geometric and material properties of the pavement structure, however, dynamic backcalculation of pavement moduli has yet to witness its widespread use due in part to a high computational cost of (visco-) elastodynamic models. More recently, the artificial neural network approach has been the subject of increasing attention (7-8) as a computationally efficient alternative for dynamic interpretation of FWD records. To fully exploit the effects of wave propagation in characterizing pavement systems, on the other hand, dynamic-back analyses often require the use of high-frequency sources (8-9) or far-field receivers (10) as a complement to the conventional FWD measurements.

In this investigation, a simple and computationally effective modification is proposed that allows the conventional elastostatic back-analyses of FWD records to perform well even when dynamic effects are significant. The technique revolves around the concepts of discrete Fourier transform and frequency response function [Bendat and Piersol (11)] as tools for developing the pre-conditioning algorithm that filters the dynamic effects from transient FWD records. With the peak (i.e. dynamic) force and deflection measurements replaced by their zero-frequency (i.e.

static) equivalents as a means to improve the consistency of an experimental input, the static backcalculation can be further performed in a traditional fashion, but free of systematic errors associated with the neglect of dynamic effects. The backcalculation results based on synthetic deflection records that assume a stiff layer at shallow depth indicate a significant improvement in the prediction of pavement moduli when the proposed modification is used. It is also shown that the peak-deflection-to-peak-force ratio for a perfect linear elastodynamic system can differ by almost 10% depending on the shape of the load pulse, an inconsistency that is circumvented in the modified backcalculation approach.

With the aid of the fast Fourier transform (FFT), the proposed algorithm can be effectively implemented on a personal computer as a pre-processor for the existing elastostatic backcalculation software. Beyond improving the in-situ characterization of flexible pavement profiles, the modification proposed can also be applied to the analysis of rigid pavement systems.

FREQUENCY-DOMAIN CHARACTERIZATION OF PAVEMENT SYSTEMS

With reference to Figure 1, the FWD test is performed by applying an impact load on the pavement surface via a 0.3m-diameter buffered loading plate and monitoring the resulting pavement deflection through a set of geophones (i.e. vertical velocity transducers). In the Figure, the deflection time history obtained by integrating the k^{th} velocity record is denoted by $w_k(t)$ ($k=1,2,\dots,N$). The source-receiver distances used in the test are commonly less than 2 meters, with the first geophone typically placed beneath the center of the loading plate.

To illustrate the dynamic nature of the pavement response to FWD excitation, typical field records of the impact force $q(t)$ and the associated surface deflections $w_k(t)$ ($k=1,2,\dots,9$) obtained at the Minnesota Road (MnROAD) research facility [e.g. Van Deusen et al. (12)] are presented in Figure 2, wherein the nine featured geophones are spaced respectively 0, 0.20, 0.30, 0.46, 0.61, 0.91, 1.22, 1.52, and 1.83 meters from the center of the loading plate. From the diagram, one may observe several prominent features of wave propagation such as (i) time delay between the load pulse and the geophone response, and (ii) free (i.e. post-peak) deflection fluctuations which signify the free vibrations of the pavement system.

On the basis of dynamic measurements such as those in Figure 2, the pavement section can be conveniently characterized in the frequency domain in terms of its *frequency response functions* (11). Upon introducing the Fourier integral transform of a temporal record $g(t)$ via

$$G(f) = \int_{-\infty}^{\infty} g(t) e^{-i(2\pi f)t} dt \quad (1)$$

whose inverse can be expressed as

$$g(t) = \int_{-\infty}^{\infty} G(f) e^{i(2\pi f)t} df \quad (2)$$

the frequency response functions (FRF's) characterizing the pavement system can be conveniently defined as

$$FRF_k(f) = \frac{W_k(f)}{Q(f)}, \quad k = 1, 2, \dots, N \quad (3)$$

where $Q(f)$ and $W_k(f)$ denote the respective Fourier transforms of the applied force signal $q(t)$ and the induced deflection $w_k(t)$. Physically, the real and imaginary parts of $FRF_k(f)$, which is in general complex-valued, can be interpreted as the respective in-phase and out-of-phase components of the vertical steady-state deflection measured by the k^{th} transducer due to a time-harmonic force acting vertically on the loading plate with frequency f .

Despite its compactness, however, Equation 3 may be of limited value in practical situations which require the use of digitized time records of finite duration. To deal with the problem, it is convenient to employ the discrete Fourier transform (DFT) of a discretized temporal variable $g(t_j)$ where $t_j = j \Delta t$ ($j=0, 1, 2, \dots, M$) which is given by

$$[G(f_m)] = \Delta t \sum_{j=1}^M g(t_j) e^{-i(2\pi f_m)t_j}, \quad m = 0, 1, 2, \dots, M \quad (4)$$

where $f_m = m \Delta f = m/(M\Delta t)$. By virtue of Equation 4, the discrete version of Equation 3 that is suitable for engineering applications can be written as

$$FRF_k(f_m) = \frac{S_{qk}(f_m)}{S_{qq}(f_m)}, \quad k = 1, 2, \dots, N, \quad m = 0, 1, \dots, M \quad (5)$$

where, for multiple FWD tests ($i=1, 2, 3, \dots, N_T$),

$$\begin{aligned} S_{qk}(f_m) &= \frac{1}{N_T} \sum_{i=1}^{N_T} [Q^*(f_m)]_i [W_k(f_m)]_i, \quad k = 1, 2, \dots, N, \\ S_{qq}(f_m) &= \frac{1}{N_T} \sum_{i=1}^{N_T} [Q^*(f_m)]_i [Q(f_m)]_i, \quad m = 0, 1, \dots, M \end{aligned} \quad (6)$$

denote the cross-spectral and power-spectral density *estimates* computed from the displacement record $w_k(t)$ and the load signal $q(t)$ with “*” denoting the complex conjugation. As shown in

Bendat and Piersol (11), Equation 5 is indispensable as a tool to minimize the effect of random noise (e.g. ambient vibrations) and measurement errors on the FRF estimates.

By means of Equation 5, the frequency response functions stemming from the temporal records in Figure 2 are calculated and plotted in Figure 3 in terms of their amplitude and phase components. From the display, the dynamic nature of the FWD load-displacement relationship should again be apparent as indicated by the pronounced variation of the FRF's with frequency, as well as the mild resonance peaks located at approximately 10 and 35 Hz.

Frequency response functions such as those shown in Figure 3 are known to contain a wealth of information about the pavement system, including an insight into the viscoelastic properties of the asphalt concrete layer and the location of bedrock or seasonal stiff layer [Foinquinos et al. (4); Magnuson et al. (5)]. As such, they have been used by a number of researchers as a basis for dynamic-based interpretation of the FWD measurements [e.g. Stubbs et al. (6), Nazarian et al. (9)].

EDUCTION OF STATIC PAVEMENT RESPONSE FROM DYNAMIC SIGNALS

Despite the advantages of dynamic FWD analyses as a basis for comprehensive pavement characterization, the elastostatic-based backcalculation techniques remain a norm in pavement engineering practice owing to their computational efficiency and simplicity of use. The conventional approach in the elastostatic interpretation of FWD measurements, however, assumes that the *peak* values of the dynamic force and deflection records can be used as a close approximation of the respective static quantities. Such an assumption has been found by a number of investigations to be a major source of systematic errors in the elastostatic backcalculation of pavement moduli [e.g. Stolle and Parvini (13)].

To highlight the problem, the static pavement response is *extracted* from the featured FWD records (see Figure 2) using the zero-frequency ordinates of the respective frequency response functions in Figure 3a, i.e. by taking

$$FRF_K^{static} = FRF_k(f_0) = \frac{S_{kq}(f_0)}{S_{qq}(f_0)}, \quad k = 1, 2, \dots, N \quad (7)$$

where $f_0 = 0$. Figure 4 compares the static deflection basin computed using Equation 7 with its conventional (i.e. dynamic) counterpart constructed from the peak force and deflection values in

Figure 2. As expected, there is a systematic discrepancy between the two estimates owing to the fact that the peak-based deflection basin is significantly affected by the dynamic nature of the FWD test.

In the comparison presented in Figure 4, it should be emphasized that the values given by Equation 7 represent the *true static* pavement response (barring any measurement errors) by virtue of the fact that the contribution of all non-zero frequencies ($f_m, m=1,2,\dots,M$) is explicitly eliminated when calculating the load-displacement relationship FRF_K^{static} . As a result, the systematic backcalculation error due to the misfit between the dynamic nature of the FWD test and the elastostatic multi-layer theory underlying conventional back-analysis can be completely eliminated by using FRF_K^{static} (in conjunction with a unit force magnitude) in lieu of the peak values of the impact force $q(t)$ and the associated surface deflections $w_k(t)$.

RESULTS AND DISCUSSION

To examine the effectiveness of the proposed approach, a parametric study is performed by applying both the conventional and the modified elastostatic backcalculation (based on Equation 7 as an input) to a set of synthetic FWD records generated using the visco-elastodynamic solution in Guzina and Nintcheu (14).

Predictive model

In what follows, the multi-layered pavement system depicted in Figure 5 will be used as a reference where E_j , ν_j , and ρ_j denote the Young's modulus, Poisson's ratio, and mass density of the j^{th} layer, respectively. Notwithstanding the decided viscoelastic nature of asphalt concrete as confirmed by numerous experimental studies [e.g. (15-16)], the top AC layer is herein simulated as elastic in order to isolate the effect of dynamic phenomena on static backcalculation.

Following the approach in (14), it can be shown by means of the Hankel integral transform and the method of propagator matrices that the surface deflection of a multi-layered pavement profile due to a normal time-harmonic force $Qe^{2\pi if t}$ acting uniformly over the circular area of radius a can be written as

$$W(r; f) = \frac{2(1 + \nu_1)Q}{\pi a E_1} \int_0^{\infty} \Omega(\xi; f) J_0(r\xi) J_1(a\xi) d\xi \quad (8)$$

where r is the radial distance from the center of the loaded area; J_n denotes the Bessel function of order n , and Ω is the kernel comprising the effects of vertical wave propagation in the layered medium that include multiple wave reflection, transmission and conversion at material interfaces. To evaluate the featured semi-infinite integral numerically, Equation 8 is recast using the method of asymptotic decomposition [Guzina and Pak (17)] as

$$W(r; f) = \Psi(r) + \frac{2(1 + \nu_1)Q}{\pi a E_1} \int_0^{\infty} \{\Omega(\xi; f) - \Omega^{as}(\xi)\} J_0(r\xi) J_1(a\xi) d\xi \quad (9)$$

where

$$\begin{aligned} \Omega^{as}(\xi) &= \lim_{\xi \rightarrow \infty} \Omega(\xi; f) = \frac{1 - \nu_1}{\xi}, \\ \Psi(r) &= \frac{2(1 + \nu_1)Q}{\pi a E_1} \int_0^{\infty} \Omega^{as}(\xi) J_0(r\xi) J_1(a\xi) d\xi \quad (10) \\ &= \frac{2(1 - \nu_1^2)Q}{\pi^2 a^2 E_1} \left[(a - r) F\left(\frac{2\sqrt{ar}}{a + r}\right) + (a + r) E\left(\frac{2\sqrt{ar}}{a + r}\right) \right] \end{aligned}$$

with $F(\dots)$ and $E(\dots)$ denoting the complete elliptic integrals of the first and second kind, respectively [see (14)]. Equation 9 effectively decomposes the dynamic deflection $W(r;f)$ into a closed-form part (Ψ) and a *residual* integral which is, owing to the rapid decay of $(\Omega - \Omega^{as})$, amenable to numerical quadrature via suitable truncation of the integration interval. In view of the existence of multiple Rayleigh wave poles (i.e. singularities) characterizing $\Omega(\xi, f)$ along the formal integration path ($0 < \xi < \infty$), the residual integral in Equation 9 is evaluated using the method of adaptive contour integration (17).

For an assumed load time history $q(t)$, transient deflection records $w_k(t)$ can be evaluated on the basis of the time-harmonic solution $W(r_k; f)$ given by Equation 9 and the inverse Fourier transform (see Equation 2).

Comparative Study

To expose the dynamic response of the pavement system featured in Figure 5 to FWD loading in the presence of a shallow stiff layer, the pavement surface deflections are simulated assuming the load time history given in Figure 6 for seven values of the subgrade thickness (h_s), namely 0.5, 1,

2, 3, 4, 5, and 6m. The spacing of nine virtual sensors that are used to represent the field measurements is taken according to the second row in Table 1 (labeled “Layout A”) wherein “Distance” represents the receiver location as measured from the center of the loading plate. As an illustration, the synthetic deflection time histories for $h_s=1\text{m}$ and $h_s=4\text{m}$ are plotted in Figure 6. For completeness, amplitudes of the respective frequency response functions that are computed from the transient records by means of Equations 4-6 are plotted in Figure 7. As can be seen from both displays, dynamic effects are more pronounced in the case of a shallower stiff layer ($h_s=1\text{m}$) as indicated by the free (i.e. post-peak) oscillations in the time domain and the resonant peak in the frequency domain. The results for all seven subgrade thicknesses are synthesized in Figures 8 and 9 wherein the composite deflection basins are generated using (i) peak values of the temporal deflection records, and (ii) zero-frequency ordinates of the respective frequency response functions stemming from Equations 4-6. Consistent with the case of field data obtained at the MnROAD research facility, there are profound differences between the peak- and FRF-based displacement profiles. In contrast to their true zero-frequency values, for instance, the peak-based deflections appear to be insensitive to the presence of a stiff layer for $h_s>2\text{m}$, a phenomenon that was also observed in Foinquinos et al. (4).

On the basis of the deflection profiles plotted in Figures 8 and 9, the pavement Young’s moduli are estimated using the elastostatic backcalculation software Evercalc 5.0 [WSDOT (18)]. In the procedure, the “true” subgrade thickness (h_s) that is used to simulate the measurements is made available to the program. For completeness, the seed moduli and their respective upper and lower limits used in the back-analysis are listed in Table 2. One may observe that the seed values for the backcalculation based on peak deflections are taken to be equal to the “true” pavement moduli in order to prevent the conventional inverse solution from being trapped into a local minimum.

The backcalculation results are compared in Figures 10 and 11 wherein the estimates of the pavement’s Young’s moduli based on the peak- and FRF-based deflection values are denoted as “Evercalc” and “Modified Evercalc”, respectively. From the display, one may observe a marked improvement in the estimation of the pavement’s elastic moduli resulting from the modified procedure. Regardless of the depth to the stiff layer, the modified approach yields the Young’s moduli of the asphalt concrete, base, and subgrade layers within 10% of their respective true values. In contrast, the conventional elastostatic backcalculation results in a significant

prediction error for most configurations examined. With the exception of a very shallow stiff layer ($h_s=0.5\text{m}$), the peak deflection-based analysis consistently (i) overestimates the stiffness of the asphalt concrete and base layers, and (ii) underestimates the subgrade and half-space moduli, often reaching the limiting modulus values given in Table 2.

Sensitivity of static deflections to the presence of stiff layer

From Figure 11b, one may observe that the FRF-based backcalculation analysis, despite its advantages, fails to yield accurate predictions of the modulus of the stiff layer for subgrade thicknesses larger than 2 meters. Owing to the fact that the principal source of systematic errors (caused by the neglect of dynamic phenomena) has been eliminated in the modified approach, it appears that such lack of resolving power is a result of the limited source-receiver spacing (Table 1, Layout A) that is used to provide an input to the back-analysis. For instance, it was found in Meier and Rix (7) that the FWD deflection basins are practically insensitive to the presence of bedrock for all depths in excess of approximately 3m, which implicitly explains the backcalculation performance in Figure 11b.

To substantiate the foregoing argument, transient FWD records for the synthetic pavement profile in Figure 5 are complemented with the aid of an *additional* virtual sensor placed 3.5m from the center of the loading plate (see Layout B in Table 1). From Figure 12 which plots the estimates of the half-space modulus based on the extended sensor layout, it can be seen that the addition of a remote sensor clearly improves the resolution of the modified approach for larger depths to the stiff layer. From numerical simulations, however, it was concluded that an accurate elastostatic-based characterization of the stiff layer at significant depths requires the use of additional remote sensors, whereas the number of geophones in this study was limited to 10 by the backcalculation software used. From the display, it should also be observed that the use of the extended sensor layout brings virtually no improvement to the conventional backcalculation analysis, a result that is consistent with the demonstrated insensitivity of dynamic deflection basins to the stiff layer in Figure 8.

Invariance of deflection basins under dynamic loads

To highlight the usefulness of using zero-frequency ordinates of the frequency response functions (Equation 7) as a basis for the elastostatic-based backcalculation of pavement moduli,

it should be noted that $FRF_k(f)$ in general, and therefore FRF_k^{static} are *invariants* of any linear pavement system regardless of the shape of the load pulse that is used to provide an input to the system (12). In contrast, the peak-deflection-to-peak-force ratio is, even for a perfect linear system, *dependent* on the forcing time history. As an illustration, the dynamic (i.e. peak-based) deflection basins of the synthetic pavement profile in Figure 5 with $h_s=3\text{m}$ are simulated using five distinct load pulses (see Figure 13) recorded at the MnROAD testing facility. From the resulting profiles in Figure 14, it is evident that the normalized peak deflections of a pavement system can differ by as much as 8% depending on the shape of the load pulse, even in the absence of errors due to extraneous noise and nonlinear (or viscoelastic) material behavior. It is important to observe that such discrepancy is *not* a result of numerical error associated with the DFT computation; rather, it stems from the variable participation of deflection harmonics used in calculating the peak displacement values as driven by the (variant) Fourier amplitude spectrum of the load signal.

CONCLUSIONS

In this investigation, a simple, yet effective technique is proposed as a means to improve the elastostatic-based backcalculation of pavement moduli from Falling Weight Deflectometer measurements. In the technique, the frequency response functions characterizing the pavement system are used as a pre-processing tool that filters the dynamic effects and extracts the static pavement response from transient FWD records. With the use of the zero-frequency force and deflection values in lieu of their peak (i.e. dynamic) counterparts, conventional static backcalculation can be further performed in a conventional manner, but free of systematic errors associated with the neglect of dynamic phenomena. It is shown that the proposed technique further improves the consistency of elastostatic pavement diagnosis owing to the invariance of the frequency response functions characterizing a linear system under varying dynamic excitation. Numerical results including a stiff layer at shallow depth indicate a marked improvement in the elastostatic backcalculation results when the foregoing modification is used. With the aid of the fast Fourier transform, the proposed alteration can be implemented on a personal computer as a pre-processor to the conventional backcalculation software with a minimal increase in computational time.

Despite the consistency it brings to the elastostatic-based backcalculation, however, the proposed technique is not intended to serve as a replacement for the dynamic analyses of FWD measurements. In fact, by the very process of educting the static pavement response from the transient force and deflection signals, the proposed approach eliminates the wealth of information about the pavement system that could otherwise be used to enhance the backcalculation results. One such example is a limited sensitivity of the elastostatic back-analyses to the presence of a stiff layer at moderate to large depths, where the dynamic backcalculation algorithms could clearly provide a better resolution by exploiting the resonance phenomena embedded in the FWD response. Another is the inherent inability of static backcalculation to resolve the frequency-dependent moduli of asphalt concrete layer and thus fully characterize its viscoelastic nature.

ACKNOWLEDGMENT

The support of the National Science Foundation through CAREER award CMS-9875495 during the course of this investigation is gratefully acknowledged.

REFERENCES

1. Davies, T. G., and M. S. Mamlouk. Theoretical Response of Multilayer Pavement Systems to Dynamic Nondestructive Testing. *Transportation Research Record 1022*, TRB, National Research Council, Washington, D.C., 1985, pp. 1-7.
2. Roesset, J. M., and K. Shao. Dynamic Interpretation of Dynaflect and Falling Weight Deflectometer Tests. *Transportation Research Record 1022*, TRB, National Research Council, Washington, D.C., 1985, pp. 7-16.
3. Uzan, J. Dynamic Linear Back Calculation of Pavement Material Parameters. *ASCE Journal of Transportation Engineering*, Vol. 120, No. 1, 1994, pp. 109-126.

4. Foinquinos, R., J. M. Roesset, and K. H. Stokoe, II. Response of Pavement Systems to Dynamic Loads Imposed by Nondestructive Tests. *Transportation Research Record 1504*, TRB, National Research Council, Washington, D.C., 1996, pp. 57-67.
5. Magnuson, A. H., R. L. Lytton, and R. C. Briggs. Comparison of Computer Predictions and Field Data for Dynamic Analysis of Falling Weight Deflectometer Data. *Transportation Research Record 1293*, TRB, National Research Council, Washington, D.C., 1991, pp. 61-71.
6. Stubbs, N., V. S. Torpunuri, R. L. Lytton, and A. H. Magnuson. A Methodology to Identify Material Properties in Pavements Modeled as Layered Viscoelastic Halfspaces (Theory). In *Nondestructive Testing of Pavements and Backcalculation of Moduli, Second Volume* (Harold L. Von Quintas, Albert J. Bush, III, and Gilbert Y. Baladi, eds.), ASTM STP 1198, ASTM, Philadelphia, Pa., 1994, pp. 361-379.
7. Meier, R. W., and G. J. Rix. Backcalculation of Flexible Pavement Moduli From Dynamic Deflection Basins Using Artificial Neural Networks. *Transportation Research Record 1473*, TRB, National Research Council, Washington, D.C., 1995, pp. 72-81.
8. Kim, Y., and Y. R. Kim. Prediction of Layer Moduli from Falling Weight Deflectometer and Surface Wave Measurements Using Artificial Neural Network. *Transportation Research Record 1639*, TRB, National Research Council, Washington, D.C., 1998, pp. 53-61.
9. Nazarian, S., M. Baker, and K. Crain. Use of Seismic Pavement Analyzer in Pavement Evaluation. *Transportation Research Record 1505*, TRB, National Research Council, Washington, D.C., 1995, pp. 1-8.
10. Aouad, M. F., K. H. Stokoe, II, and S. Joh. Estimating Subgrade Stiffness and Bedrock Depth: Combined Falling Weight Deflectometer and Simplified Spectral Analysis of Surface Waves Measurements. *Transportation Research Record 1716*, TRB, National Research Council, Washington, D.C., 2000, pp.40-48.

11. Bendat, J. S., and A. G. Piersol. *Random Data: Analysis and Measurement Procedures*. John Wiley and Sons, Inc., New York, 1996.
12. Van Duesen, D. A., C. A. Lenngren, and D. E. Newcomb. A Comparison of Laboratory and Field Subgrade Moduli at the Minnesota Road Research Project. In *Nondestructive Testing of Pavements and Backcalculation of Moduli, 2nd Volume* (Harold L. Von Quintas, Albert J. Bush, III, and Gilbert Y Baladi, eds.), ASTM STP 1198, ASTM, Philadelphia, Pa., 1994, pp. 361-379.
13. Stolle, D. F. E., and M. Parvini. A Look at Modelling Errors for Falling Weight Deflectometer Backcalculation. *Transportation Research Record* (pre-print), 80th Annual Meeting of Transportation Research Board, 2001, Washington, D.C.
14. Guzina, B. B., and S. Nintcheu. Effects of Ground-Structure Interaction in Dynamic Plate Load Testing. *International Journal for Numerical and Analytical Methods in Geomechanics*, 2001, under review.
15. Sousa, J. B., and C. L. Monismith. Dynamic Response of Paving Materials. *Transportation Research Record 1136*, TRB, National Research Council, Washington, D.C., 1987, pp. 57-68.
16. Zhang, W., A. Drescher, and D. E. Newcomb. Viscoelastic Analysis of Diametral Compression of Asphalt Concrete. *Journal of Engineering Mechanics*, ASCE, Vol. 123, No. 6, 1997, pp. 596-603.
17. Guzina, B. B., and R. Y. S. Pak. On the Analysis of Wave Motions in a Multi-Layered Solid. *Quarterly Journal of Mechanics and Applied Mathematics*, Vol. 54, No. 1, 2001, pp.13-37.
18. Washington State Department of Transportation, *WSDOT Pavement Guide*, Seattle, Washington, 1995.

LIST OF TABLES

1. Sensor locations used for computing synthetic FWD records
2. Limiting and seed values of pavement moduli used for backcalculation

LIST OF FIGURES

1. Falling Weight Deflectometer setup.
2. FWD time histories (MnROAD testing facility, June 6, 2001).
3. Frequency response functions computed from field FWD records.
4. Static and dynamic deflection basins (MnROAD, June 6, 2001).
5. Synthetic pavement profile.
6. Simulated deflection records.
7. Frequency response functions computed from simulated FWD records (amplitude).
8. Synthetic deflection basins constructed from peak values.
9. Synthetic deflection basins constructed from zero-frequency FRF values.
10. Young's moduli of the asphalt concrete and base layers estimated from synthetic FWD records (Sensor Layout A).
11. Young's moduli of the subgrade and semi-infinite stiff layer estimated from synthetic FWD records (Sensor Layout A).
12. Young's modulus of the semi-infinite stiff layer estimated from synthetic FWD records (Sensor Layout B).
13. Load pulses recorded at the MnROAD testing facility.
14. Synthetic peak deflections computed using various load pulses.

TABLE 1 Sensor locations used for computing synthetic FWD records

Sensor	1	2	3	4	5	6	7	8	9	10
Distance [m] (Layout A)	0.0	0.20	0.30	0.46	0.61	0.91	1.22	1.52	1.83	N/A
Distance [m] (Layout B)	0.0	0.20	0.30	0.46	0.61	0.91	1.22	1.52	1.83	3.5

TABLE 2 Limiting and seed values of pavement moduli used for backcalculation

Young's Modulus	AC	Base	Subgrade	Stiff layer
Max. [MPa]	8000	350	100	2000
Min. [MPa]	1000	100	10	300
Seed [MPa] (Evercalc)	3240	216	56	1160
Seed [MPa] (Modified Evercalc)	2000	180	27	500
True Value [MPa]	3240	216	56	1160

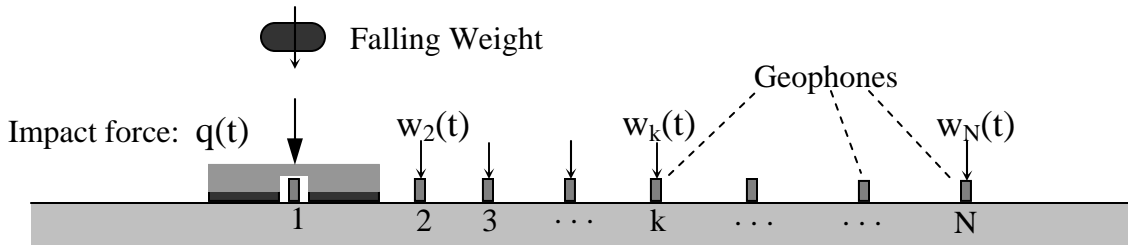


FIGURE 1 Falling Weight Deflectometer setup.

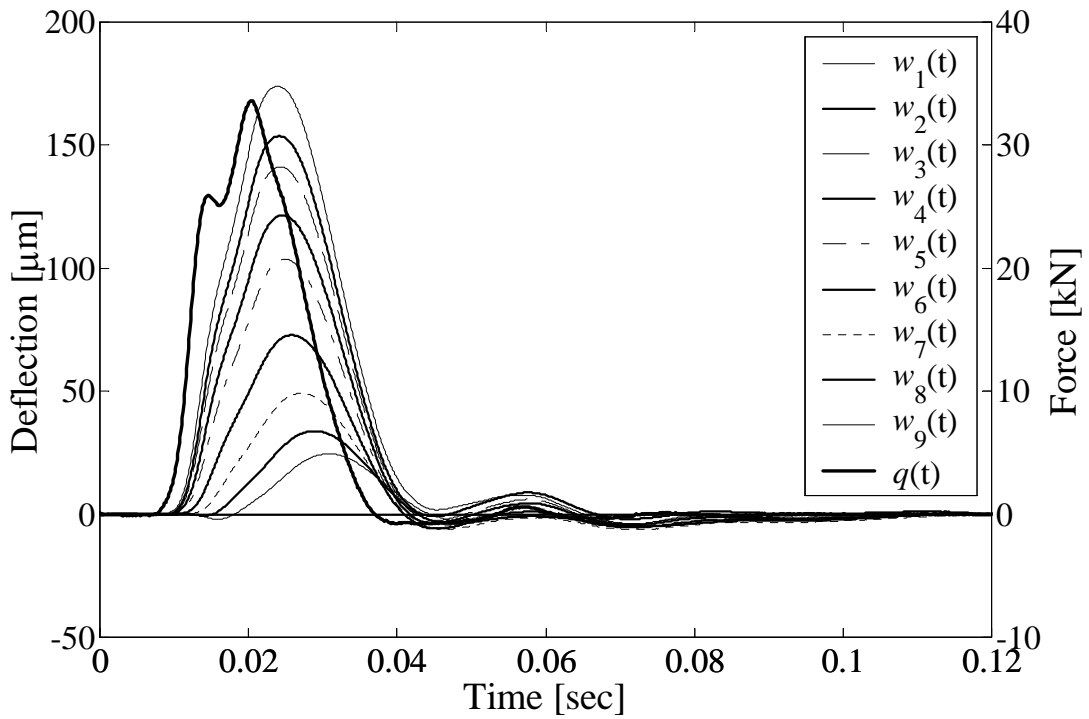


FIGURE 2 FWD time histories (MnROAD testing facility, June 6, 2001).

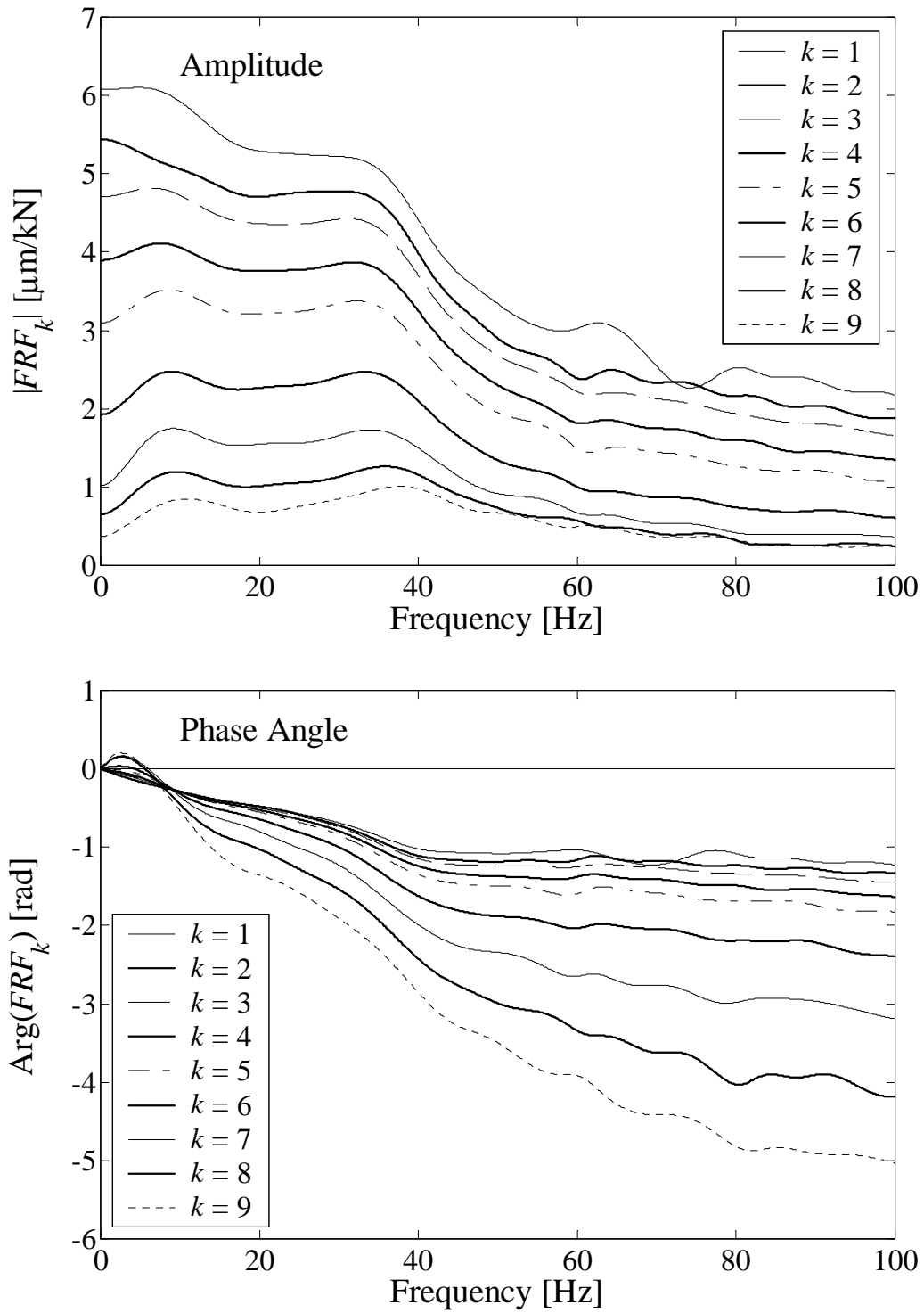


FIGURE 3 Frequency response functions computed from field FWD records.

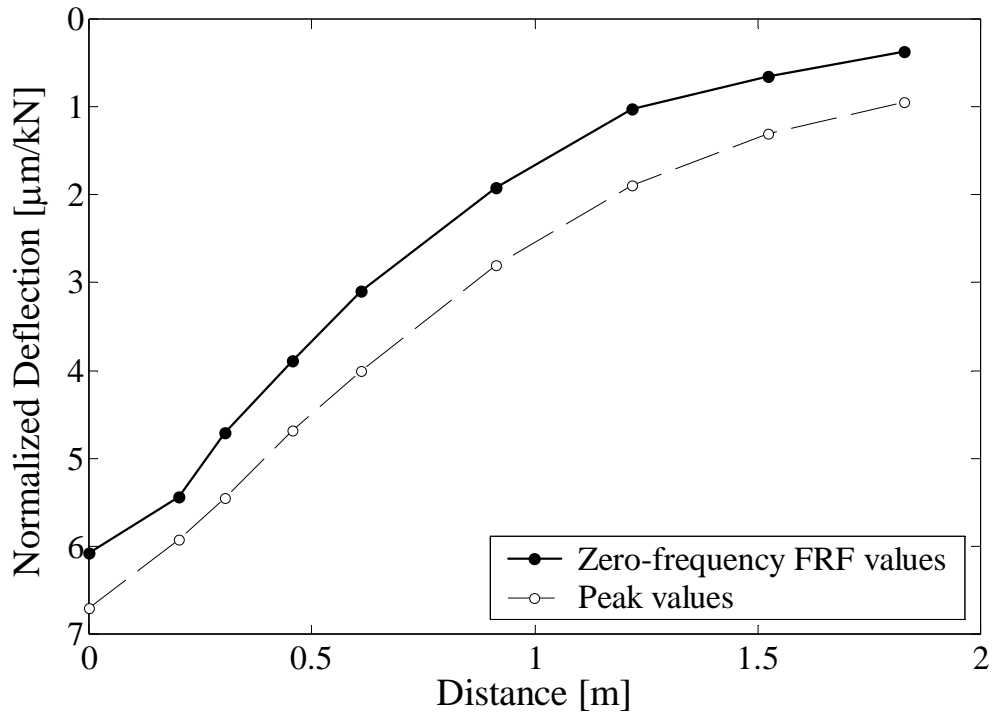


FIGURE 4 Static and dynamic deflection basins (MnROAD, June 6, 2001).

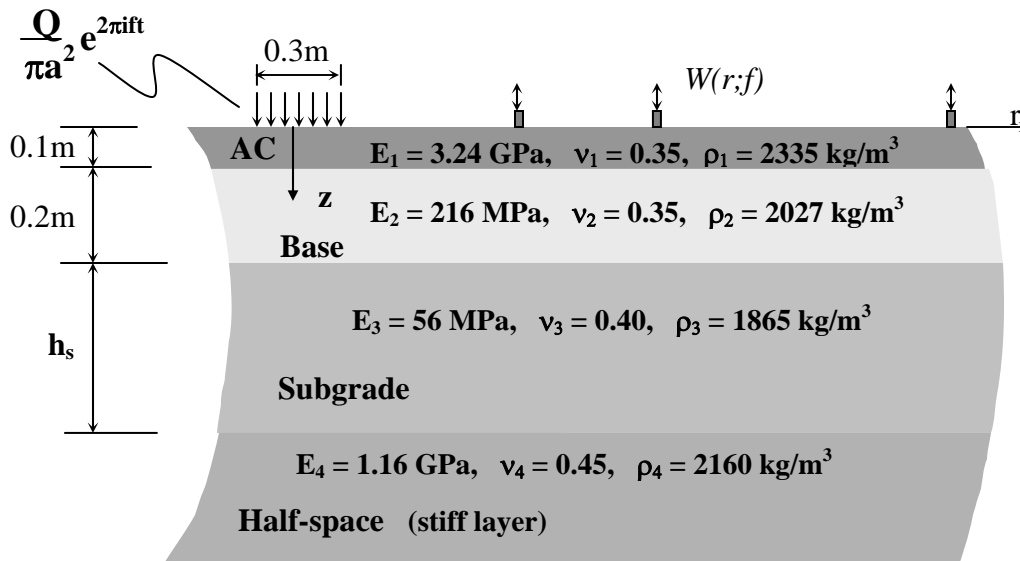


FIGURE 5 Synthetic pavement profile.

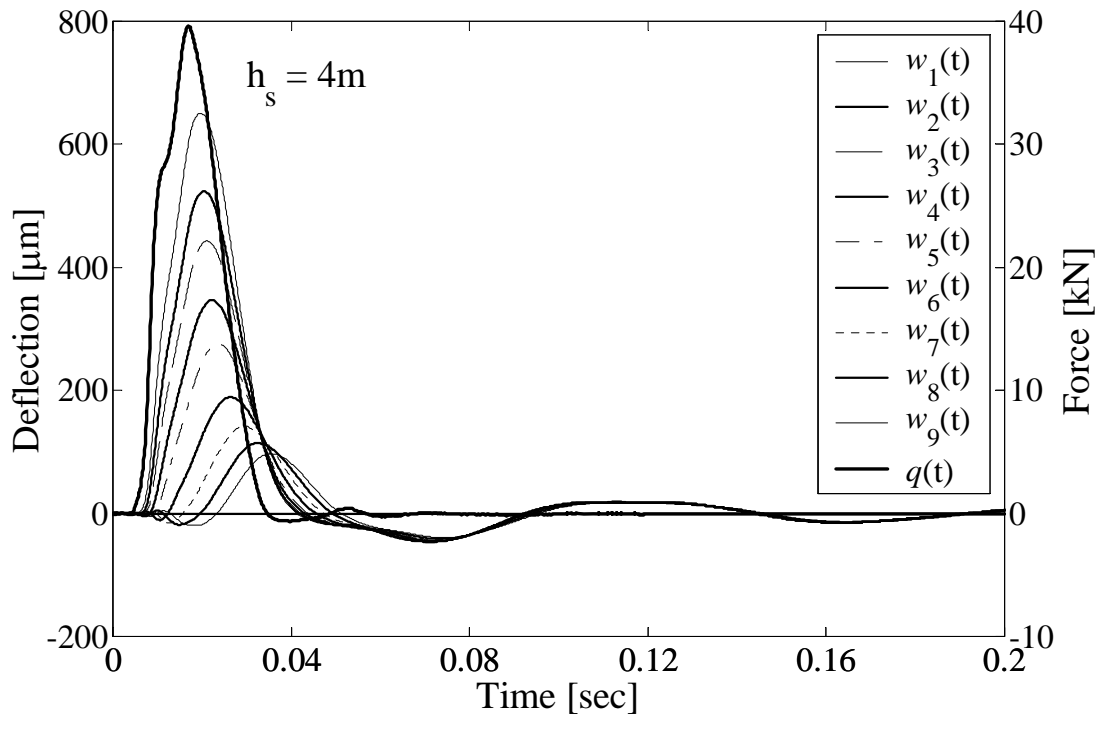
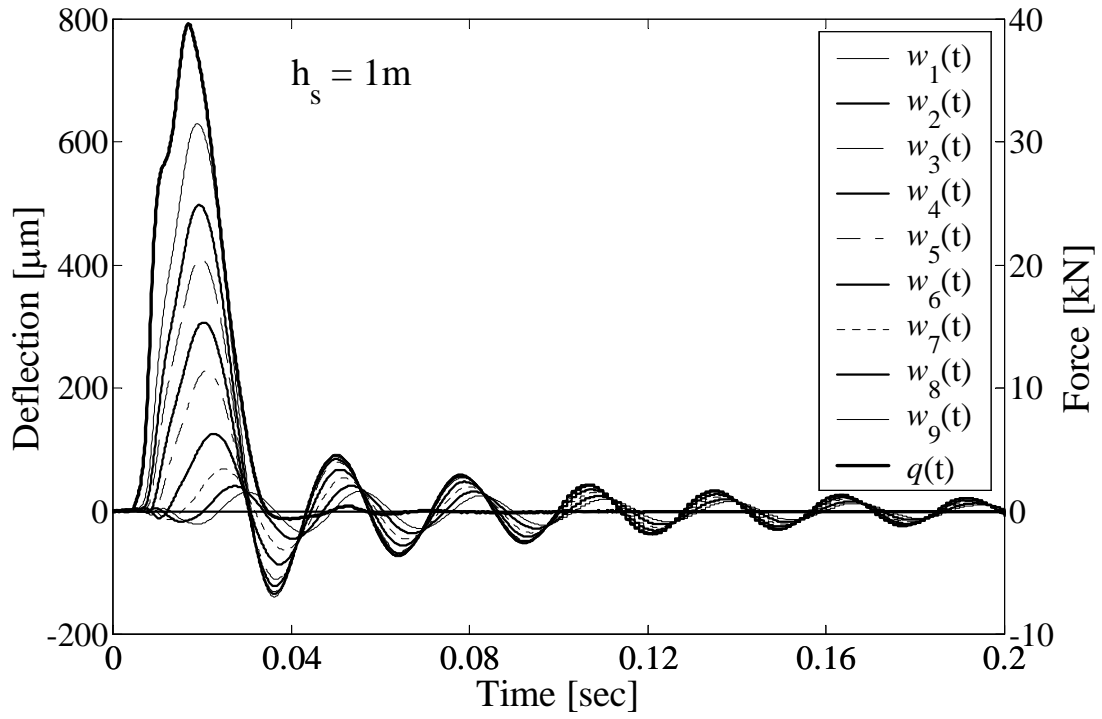


FIGURE 6 Simulated deflection records.

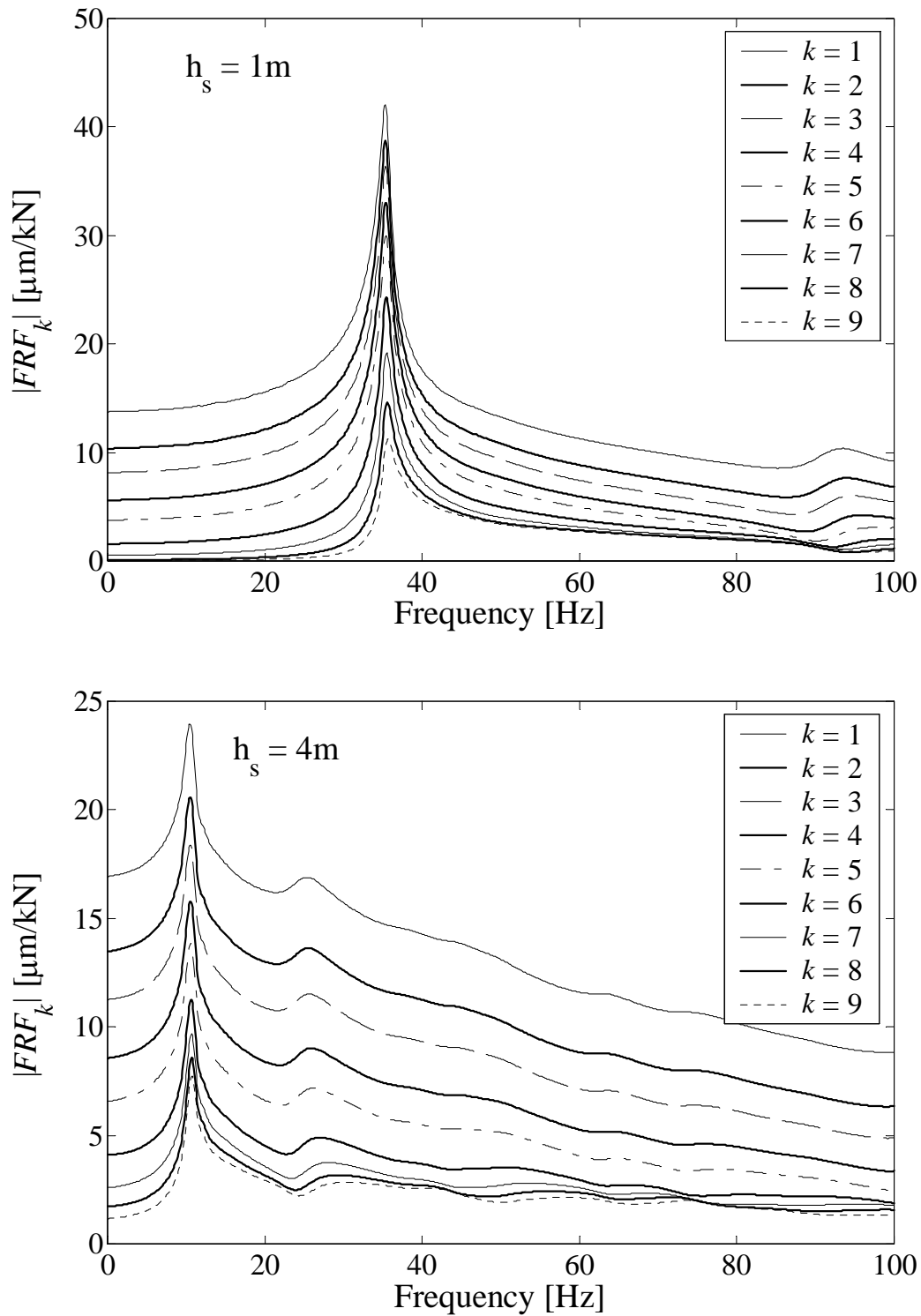


FIGURE 7 Frequency response functions computed from simulated FWD records (amplitude).

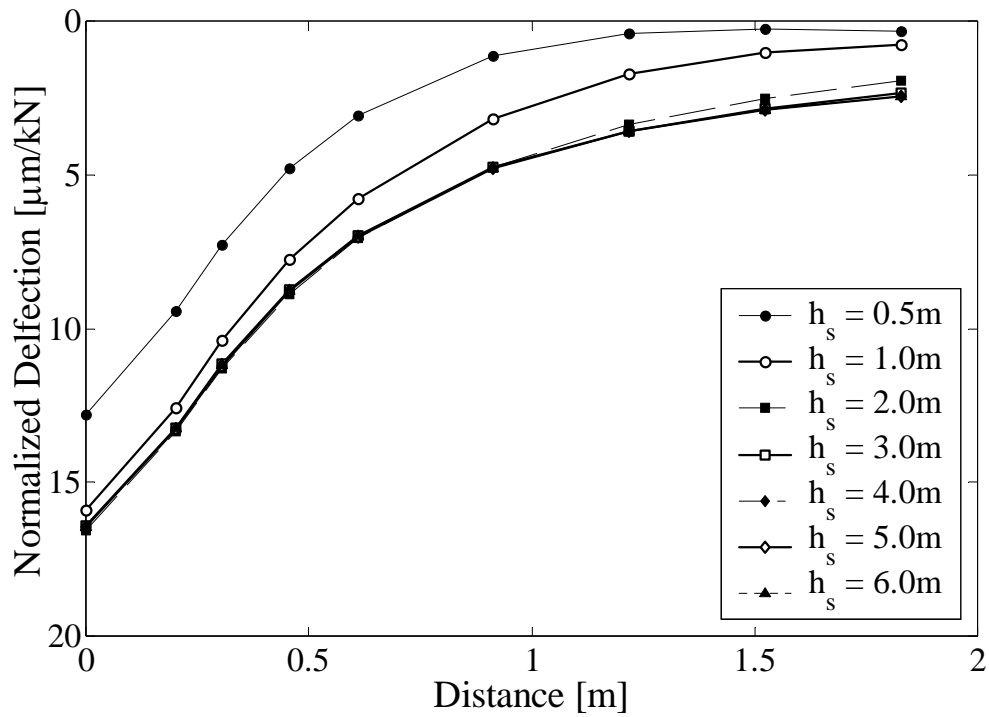


FIGURE 8 Synthetic deflection basins constructed from peak values.

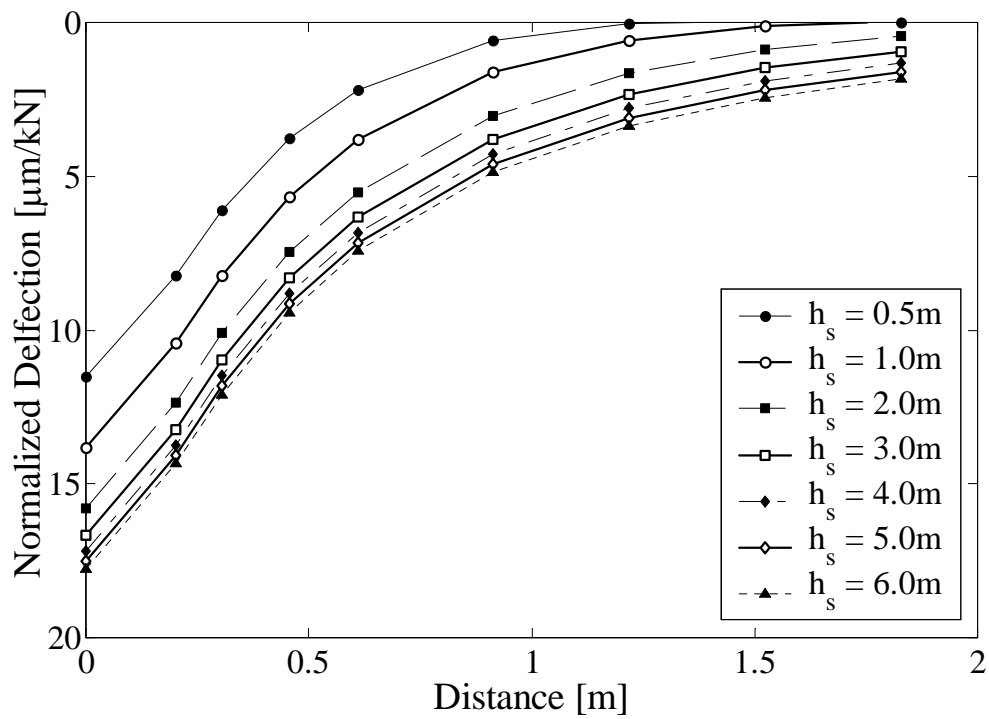


FIGURE 9 Synthetic deflection basins constructed from zero-frequency FRF values.

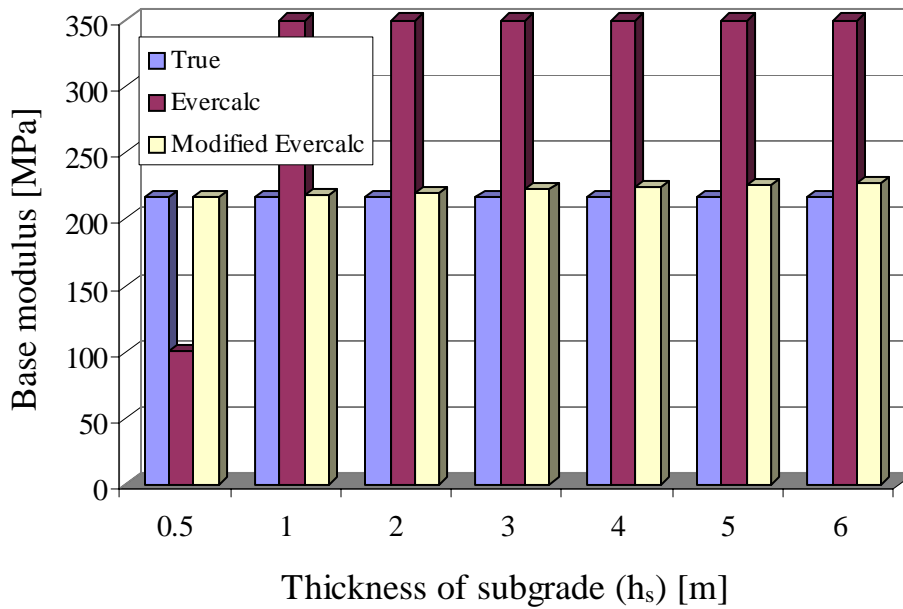
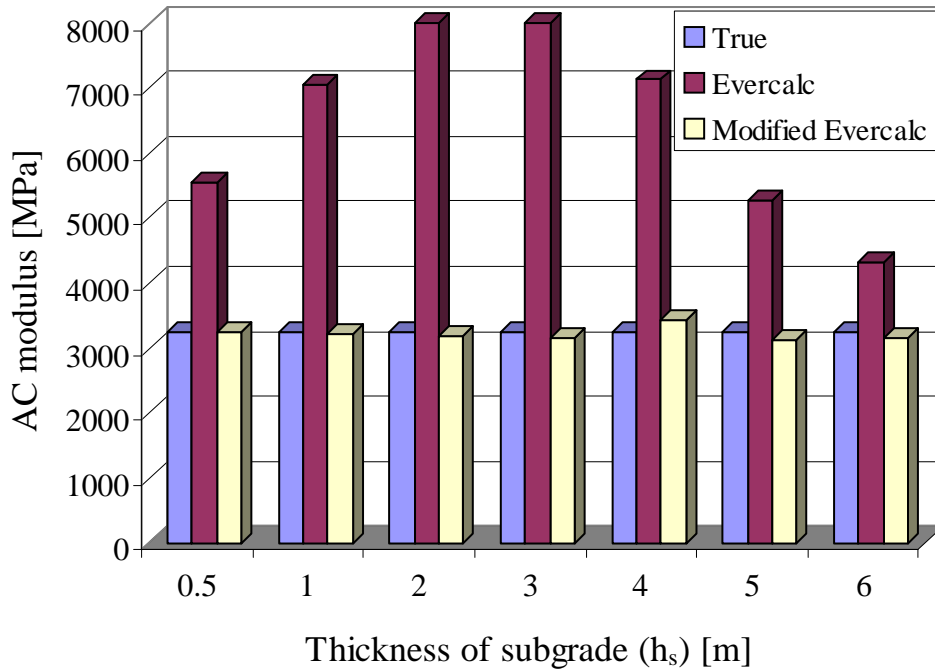


FIGURE 10 Young’s moduli of the asphalt concrete and base layers estimated from synthetic FWD records (Sensor Layout A).

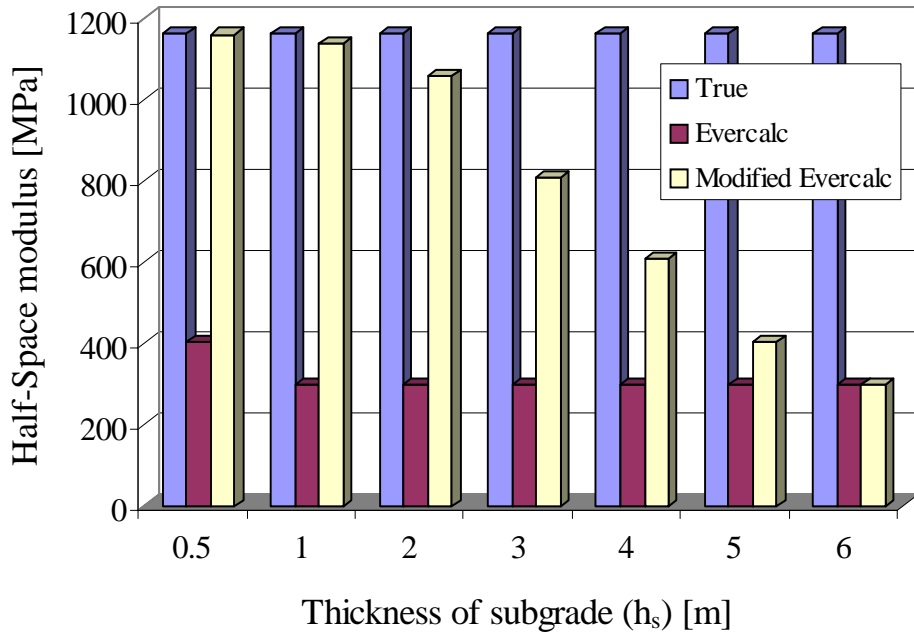
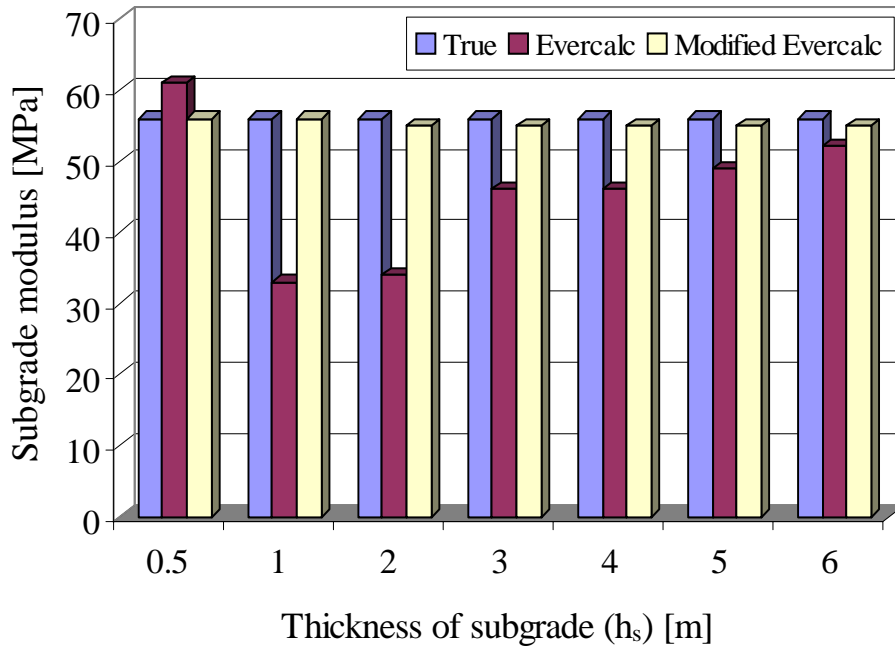


FIGURE 11 Young’s moduli of the subgrade and semi-infinite stiff layer estimated from synthetic FWD records (Sensor Layout A).

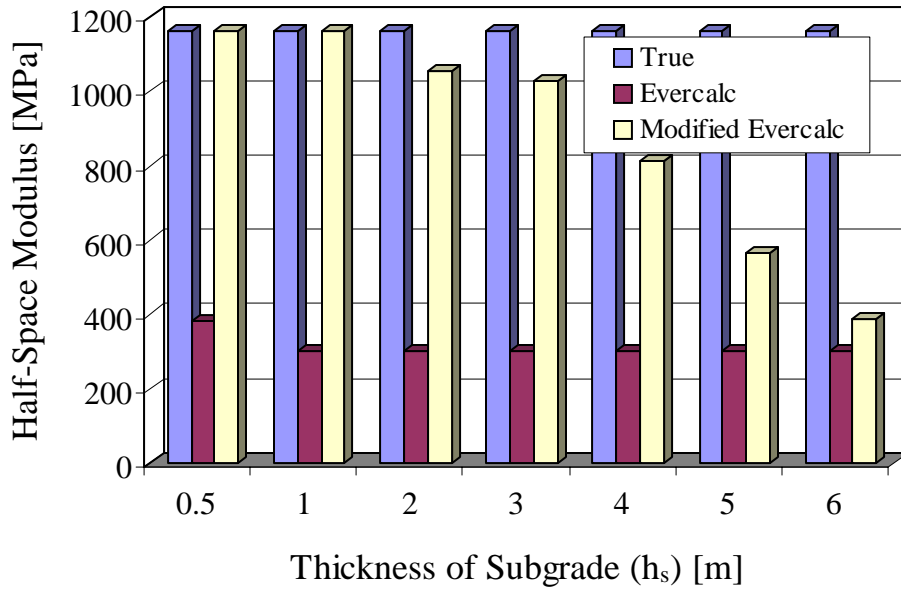


FIGURE 12 Young’s modulus of the semi-infinite stiff layer estimated from synthetic FWD records (Sensor Layout B).

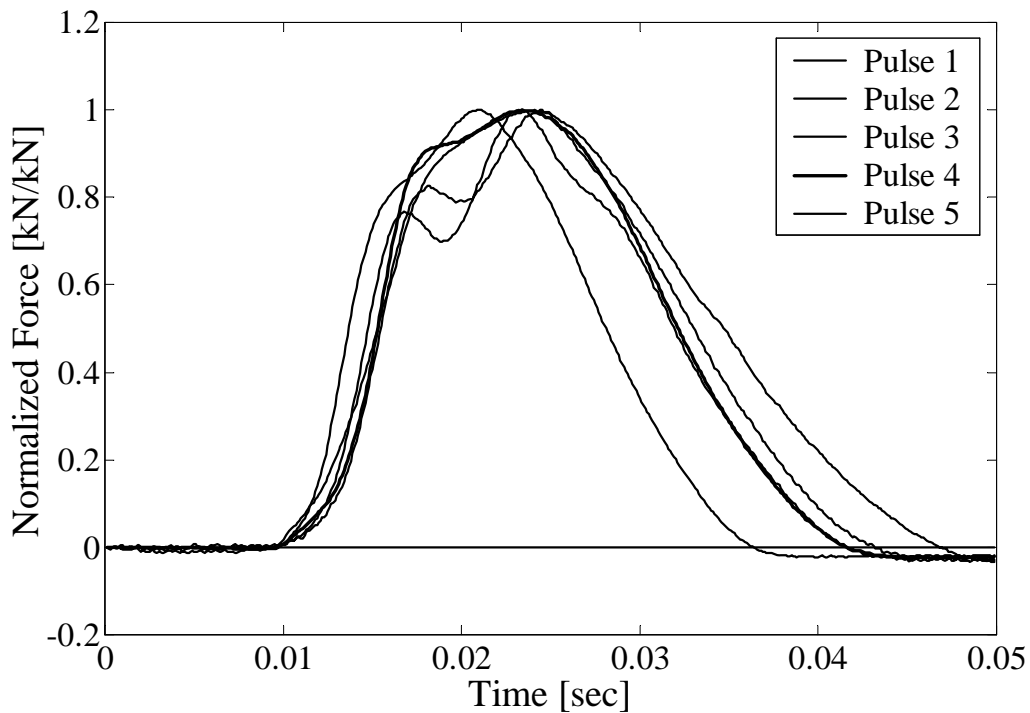


FIGURE 13 Load pulses recorded at the MnROAD testing facility.

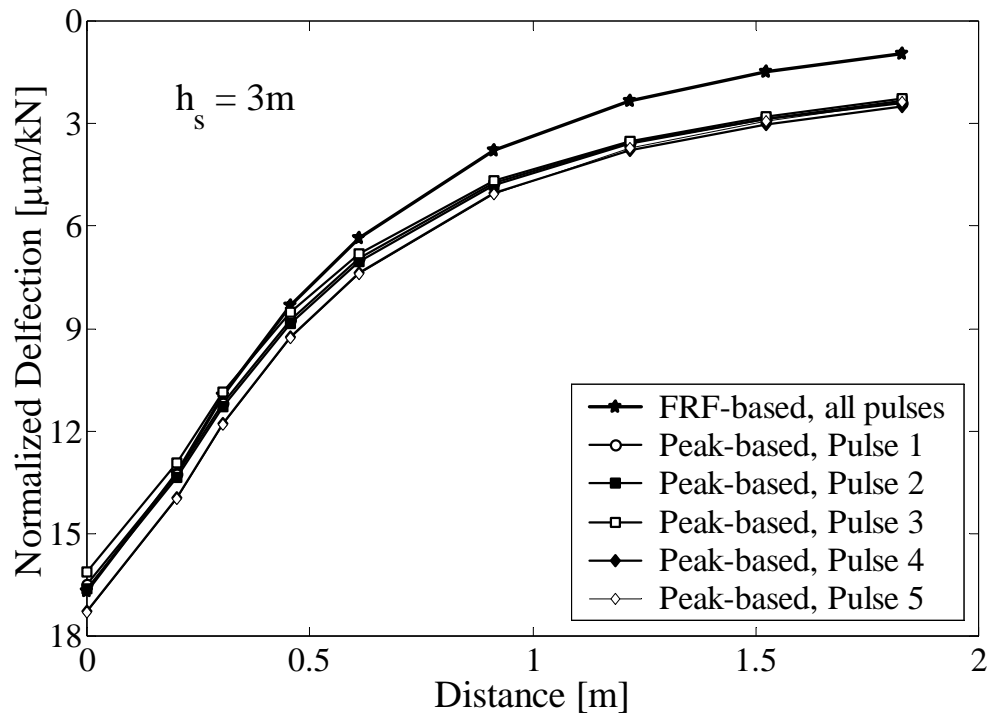


FIGURE 14 Synthetic peak deflections computed using various load pulses.